Shock initiation of explosives: High temperature hot spots explained

Will P. Bassett, Belinda P. Johnson, Nitin K. Neelakantan, Kenneth S. Suslick,[a)] and Dana D. Dlott[a)]
School of Chemical Sciences and Fredrick Seitz Materials Research Laboratory, University of Illinois at Urbana-Champaign, Urbana, Illinois 61801, USA

(Received 30 May 2017; accepted 29 July 2017; published online 10 August 2017)

We investigated the shock initiation of energetic materials with a tabletop apparatus that uses km s^{-1} laser-driven flyer plates to initiate tiny explosive charges and obtains complete temperature histories with a high dynamic range. By comparing various microstructured formulations, including a pentaerythritol tetranitrate (PETN) based plastic explosive (PBX) denoted XTX-8003, we determined that micron-scale pores were needed to create high hot spot temperatures. In charges where micropores (i.e., micron-sized pores) were present, a hot spot temperature of 6000 K was observed; when the micropores were pre-compressed to nm scale, however, the hot spot temperature dropped to ~4000 K. By comparing XTX-8003 with an analog that replaced PETN by nonvolatile silica, we showed that the high temperatures require gas in the pores, that the high temperatures were created by adiabatic gas compression, and that the temperatures observed can be controlled by the choice of ambient gases. The hot spots persist in shock-compressed PBXs even in vacuum because the initially empty pores became filled with gas created *in-situ* by shock-induced chemical decomposition. *Published by AIP Publishing*. [http://dx.doi.org/10.1063/1.4985593]

Localization of mechanical energy into the so-called hot spots is central to the process of shock initiation of energetic materials (EMs).[1] Recent pyrometry measurements of EMs with nanosecond time resolution[2–5] have shown extraordinarily high initial hot spot temperatures, up to 7500 K,[5] which seemed too high to originate from solid phase reactions of explosives, which are generally in the 2000–4000 K range.[6] In this study, we investigated the nature of these high hot spot temperatures and their dependence on the EM microstructure and gas environment.

Understanding hot spots is central to the development of safer explosives[7] and initiators.[8] The verification of theoretical studies of hot spots, working from molecular to continuum scales,[9] requires the corresponding experimental measurements of temperature, pressure, and chemical reactivity as a function of the microstructure.[10,11] We have recently developed an experimental platform that allows us to measure thermal histories of microgram explosive charges with nanosecond temporal resolution during initiation by km s^{-1} aluminum flyers,[2,3] and we used this platform to study hot spots in an impact-initiated plastic-bonded explosive (PBX) formulation having micro- and nanopores filled with various gases. The fabricated PBX has the same composition as the commercial pentaerythritol tetranitrate (PETN)-based explosive XTX-8003 (hereafter abbreviated as XTX).[12,13]

An important hot spot formation mechanism is adiabatic compression of gas in a collapsing pore.[14] The hot spot peak temperatures depend on the way the sample microstructure responds to the impact and the gas composition in the pore.[14] Molecular simulations of pore collapse typically involve nanometer-scale voids where atoms were removed from the specified geometry, leaving behind vacuum,[15–19] whereas experiments mostly look at EM with air-filled pores.[14,20] In shock experiments, pores held under nominal vacuum become filled with gases, and primarily, gases evolved from the shocked and heated EM and binder materials. Molecular dynamics simulations have showed that the chemical decomposition of shocked EM can produce gases within picoseconds, faster than the pore can collapse.[21–24]

Our experimental arrangement is depicted schematically in Fig. 1(a) and has been described elsewhere in detail.[3,4] The EM samples were placed in a shock target microarray, produced by placing a 38 μm thick Kapton tape with an array of 187 holes with a diameter of 1 mm on a borosilicate glass window. XTX composed of 80 wt. % PETN and 20 wt. %

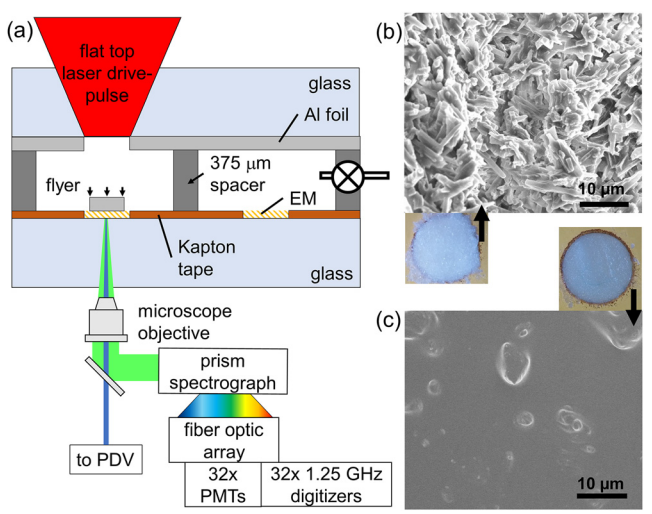

FIG. 1. (a) Schematic of the experiment (not to scale). Tiny energetic material (EM) charges of XTX-8003 (hereafter XTX) were fabricated in an array of 38 μm deep, 1 mm diameter wells. The glass substrate was $75 \times 75 \times 6.35\,mm^3$. The Al foil was 25 μm thick. (b) and (c) Electron micrographs and optical images of (b) μXTX and (c) nXTX. Note the significant microstructure change upon homogenization in a hydraulic press.

[a)]Authors to whom correspondence should be addressed: ksuslick@illinois.edu and dlott@illinois.edu

poly(dimethylsiloxane) (PDMS, Sylgard 182) was made by diluting PDMS in hexanes with a suspension of fine-grain PETN and stirred for 24 hours until the hexanes evaporated and PDMS was cured. Infrared spectroscopy was used to verify that no residual hexanes were present. Some XTX samples were used as produced and contain micron sized pores as discussed below. These samples will be referred to as microporous XTX (μXTX). The rest of the XTX was transferred to a hydraulic press where it was repeatedly flattened and folded onto itself until a homogenous putty was formed. The homogenizing process eliminated the micro-scale pores but likely left behind nanopores, and we will refer to those samples as nXTX. Differential scanning calorimetry (PYRIS Diamond, PerkinElmer) showed exotherms consistent with the literature for both μXTX and nXTX. The density of nXTX was $99 \pm 2\%$ of the reported density of XTX8003 (1.556 g cm^{-3}), while the density of μXTX was $93 \pm 4\%$ of XTX8003. Densities were determined from the mass needed to fill 3 mm diameter $\times$ 0.5 mm deep wells. Scanning electron microscopy (SEM) images of the micro- and nanoporous XTX are shown in Figs. 1(b) and 1(c). The μXTX [Fig. 1(b)] shows many micron-scale pores and has a highly scattering appearance, while nXTX [Fig. 1(c)] has a translucent appearance. Nanopores cannot be seen at the spatial resolution of these images ($\sim$1 μm), but we infer their presence from experimental results presented below. Higher resolution SEM at higher magnification to directly observe nanopores was precluded by the onset of beam damage and space charging effects. The size distribution of PETN crystals, from SEM images analyzed with the ImageJ software package, showed average crystallite sizes of 2.3 ± 1.4 μm in nXTX and 6.6 ± 2.9 μm in μXTX.

Several other types of samples were studied. Pure PETN was used in the form of loosely compacted fine powder, which is necessarily highly microporous, and in the form of vapor-deposited films 40 μm thick with an average density of $\sim$90% theoretical maximum, which were made by physical vapor deposition on *poly*(methyl methacrylate) substrates at Sandia National Laboratories.[25,26] The vapor-deposited PETN was also microporous based on electron micrographs from Sandia National Laboratories.[26] Inert homogenized PBX-analogues were made by replacing PETN with fine-grain sucrose (XTSucrose) or monodispersed 5 μm SiO_2 powder ($XTSiO_2$), i.e., both were 20% PDMS by weight. The sucrose, from Sigma Aldrich, was ground and sieved to remove particles >40 μm, and the silica from Sigma Aldrich was monodispersed 5 μm microbeads. All samples, except the vapor-deposited PETN, were loaded into the microarray wells, pressed flat by using a Teflon-coated spatula.

Laser-launched Al 1100 flyer plates 0.5 mm in diameter and 25 μm thick produced steadily driven planar impacts[27] lasting 4 ns at velocities from 1.2 to 3.2 km s^{-1}.[28] Time zero was defined, so shocks exited the XTX samples at 10 ns. Flyer velocities and impact times were measured with a high-speed photon Doppler velocimeter (PDV).[28] Data were obtained in all cases with a minimum of two separate runs where variables such as the impact velocity and gas mix were measured with a minimum of five shots. Vacuum atmosphere measurements were made by evacuating the sample chamber to less than 200 mTorr for at least 15 minutes. When the sample pores were loaded with different gases, the chamber was pumped out and back-filled with one atmosphere of gas and was flushed between shots to remove EM product gases. Gas exchange was facilitated by the high gas diffusivity of PDMS.[29] When flyers were launched in gas-filled chambers, the flyer compression of the fill gas produced a bright flash. To shield this bright flash from the pyrometer, a 500 nm thick Ti light shield was evaporated on each sample impact surface.

Data analysis algorithms, including logarithmic time-binning, gray body analysis, and a spatially averaged emissivity model, have been discussed elsewhere.[4] The emission was calibrated against a NIST-traceable source to give the gray body temperature and emissivity (Φ) as a function of time. Since sample emission was spatially inhomogeneous when hot spots were present, the measured emissivity represents a spatial average.[2–4] Large-scale changes in the sample emissivity are indicative of shock-induced chemical transformations. Data points acquired at 1.25 GHz were displayed after binning in log(time) using 15 points per decade.[4]

Figure 2(a) shows a representative thermal history of nXTX with a 2.3 km s^{-1} impact. The spectral radiances at all times were, as in previous works, good fits to a graybody model.[2,3] As a point of reference, a 2.8 km s^{-1} flyer plate impact will produce a shock at about 7.1 km s^{-1}, close to the detonation velocity of XTX-8003.[12] The temperature during the first few nanoseconds was $\sim$4000 $\pm$ 400 K, decaying to a

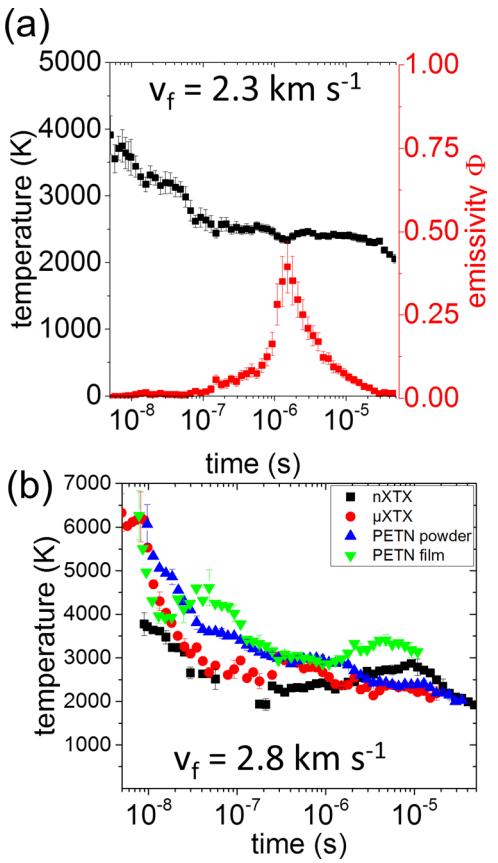

FIG. 2. (a) Thermal history and emissivity of nXTX with the 2.3 km s^{-1} impact. The initial hot spot temperature was $\sim$4000 K, and the later deflagration temperature was $\sim$2500 K. (b) Thermal histories with 2.8 km s^{-1} impacts of three microporous PETN-based samples have a hot spot temperature of $\sim$6000 K, while the nanoporous nXTX has $\sim$4000 K hot spots.

plateau of ~2500 K by about 100 ns. Within experimental error, the initial temperatures did not change with the impact velocity between 2.3 and 2.8 km s^{-1}. According to our assignment,[2,3] the initial temperature originates from hot spots, and the later temperature, which occurred after the shock unloaded, was the deflagration temperature. The emissivity of nXTX [Fig. 2(a)] showed only a single peak which resulted from deflagration. This behavior differs from previous work on finely powdered HMX (octahydro-1,3,5,7-tetranitro-1,3,5,7-tetrazocine),[2,3] where in addition to the deflagration peak there was an emissivity peak at a few nanoseconds. The lack of a nanosecond emissivity peak in nXTX indicates a much smaller combined volume of hot spots than in the HMX powder. Additionally, HMX demonstrated a temperature spike several hundred ns after impact, which was absent in the PETN-based charges studied here. The lack of secondary temperature spike is likely due to the relatively high oxygen balance of PETN, which causes the energy release to occur very quickly and without much soot formation.[30,31]

Figure 2(b) compares the thermal histories of various microporous PETN-based samples with nXTX using the 2.8 km s^{-1} impact. With nXTX, the initial hot spot temperature was ~4000 K, but with all the microporous samples, the hot spots were ~6000 K. The deflagration temperature of ~2500 K was about the same for all these samples.

Figure 2(b) demonstrates that the ~6000 K hot spots must be associated with micropore collapse, which cannot occur in nXTX where the initial microporosity was minimized by hydraulic pressing. We previously observed such an initial hot spot temperature of ~6000 K in powdered HMX.[2,3] As discussed below, the high temperature hot spots originate from gas compression not from the solid. Molecular simulations of pore collapse emphasize heat produced from the solid, but in most simulations, there is no gas. The heat from the solid originates from viscoplastic heating of the solid, chemical reactivity, and compressional heating.[15,16,18,22] However, gas in collapsing pores should get much hotter than the solid because gas is so much more compressible.[14] The importance of gas compression over solid-state heating has been supported by direct calculations. As an example, Baer *et al.* calculated the temperature of gas and solid for the compression of gas-filled micron diameter pores.[32] The gas temperature was ~5000 K, while the solid temperature was 1400 K at the gas-solid interface and lower elsewhere.

To understand whether, with the sample in vacuum, the gas in the pores originated from the shocked PETN, we compared control samples XTSucrose and $XTSiO_2$ to nXTX. PETN under shock is volatile and explosive, sucrose is less volatile and nonexplosive, and silica is nonexplosive and nonvolatile. The thermal histories and emissivities from these measurements, with an impact velocity of 2.7 km s^{-1}, are shown in Fig. 3. In the first few nanoseconds when hot spots were created, the nXTX and XTXSucrose had hot spots at ~4000 K, while $XTSiO_2$ showed negligible nanosecond time scale emission, implying the absence of any volatiles to produce hot spots. As the shorter-time emissivities in Fig. 3 show, the weaker emissivity from XTSucrose indicated a lesser number of hot spots due to the lower reactivity of

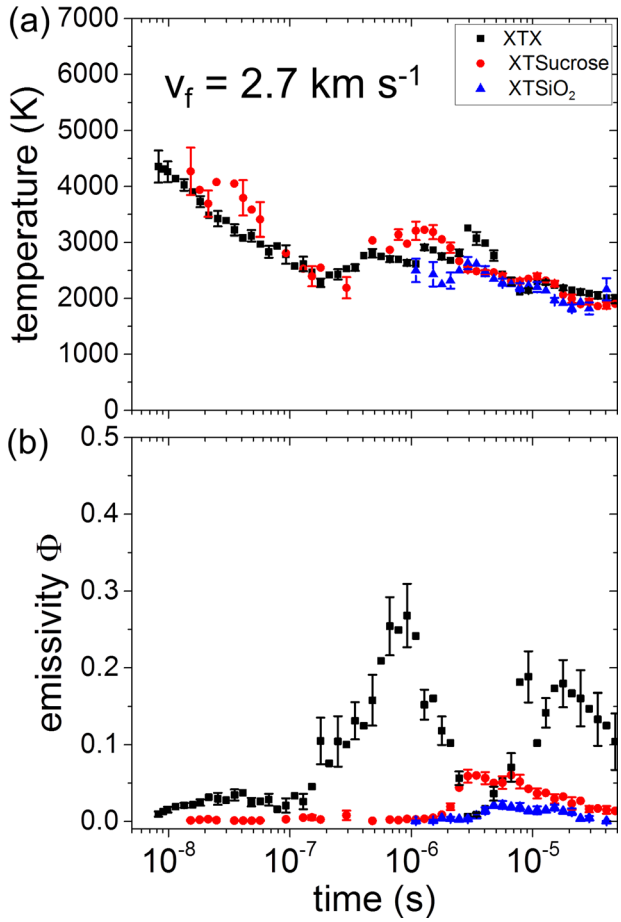

FIG. 3. Thermal histories (a) and (b) emissivities of nXTX with the volatile explosive PETN, XTSucrose with less volatile nonexplosive sugar, and $XTSiO_2$ with nonexplosive nonvolatile silica particles. The shorter-time (nanosecond) emissivities indicate that hot spots were present in greater quantities with nXTX than with XTSucrose and were essentially absent with $XTSiO_2$. The emissivity increase starting near 200 ns indicates a thermal explosion of the nXTX, which was absent with the nonexplosive samples. Weak emission in $XTSiO_2$ after several microseconds was from the glass substrate. Gaps in the data stream indicate times when the signals were too weak to accurately determine temperatures.

sucrose. nXTX had a peak in the thermal history near 2 μs not present in the other nonexplosive samples, so that the peak can be assigned to PETN deflagration. The weak emission at 10 μs and beyond in $XTSiO_2$ and XTSucrose does not result from energetic chemistries. As discussed previously,[33] it can be attributed to triboluminescence from the glass substrate.

The emissivity results in Fig. 3 show that the volume of hot spots in the collapsing pores was the largest for nXTX, smaller for XTSucrose, and negligible for nonvolatile $XTSiO_2$. This result shows that the high hot spot temperatures we observed in nXTX8003 did not originate from residual gas left over after evacuating the sample chamber but rather from gas evolved by the shock-induced decomposition of volatile species such as PETN, to a lesser extent sucrose, and possibly PDMS.

To investigate the role of the gas compressed in the pores in producing hot spots, we did experiments with pores filled with different gases. As a rough approximation, shock heating with different gases may be simply modeled by the well-known equation for adiabatic reversible heating of an ideal gas

$$\left(\frac{T_2}{T_1}\right) = \left(\frac{V_1}{V_2}\right)^{(\gamma-1)}, \quad (1)$$

where T_1, T_2, V_1, V_2, and $\gamma = C_p/C_v$ are the initial temperature, final temperature, initial volume, final volume, and specific heat ratio.[14] Equation (1) for a reversible compression neglects the additional heat from irreversible shock compression and so establishes only a lower limit for the final gas temperature T_2. The gases were chosen to span a range of γ: argon (1.6), oxygen (1.4), nitrogen (1.4), carbon dioxide (1.3), acetylene (1.2), and butane (1.1). For polyatomic gases, C_p approaches C_v, so γ approaches unity as the molecules become larger, and there are more vibrational states to soak up the shock energy.[14] These values of γ are at NTP and will differ from the effective γ under shock. During rapid changes in conditions, such as during shock compression, all vibrational modes cannot be excited, and thus, a higher value of γ might be expected.[14] Conversely, a lower γ can be expected for species initially at high temperature.[34]

Figure 4 compares thermal histories for nXTX with different fill gases and nominal vacuum. The hot spot temperature with Ar was the highest, ~6500 K, which may be even higher due to the limited sensitivity of our pyrometer in the UV. The hot spot temperature with air, O_2, N_2, and CO_2 was ~5500 K. The hot spot temperature with vacuum, acetylene, and butane was ~4000 K. Experiments in Ar, O_2, N_2, and CO_2 are consistent with the compression of species with an effective γ of $\geq$1.4, while experiments with acetylene, butane, and nominal vacuum are consistent with an effective γ of <1.4. The lower effective γ of decomposition products does not necessarily preclude di- or triatomic intermediates but suggests that they may be formed at high temperature such as would be expected for molecules formed under the shock-induced decomposition[35] or impact from molecular spall across a collapsing void.[19,36]

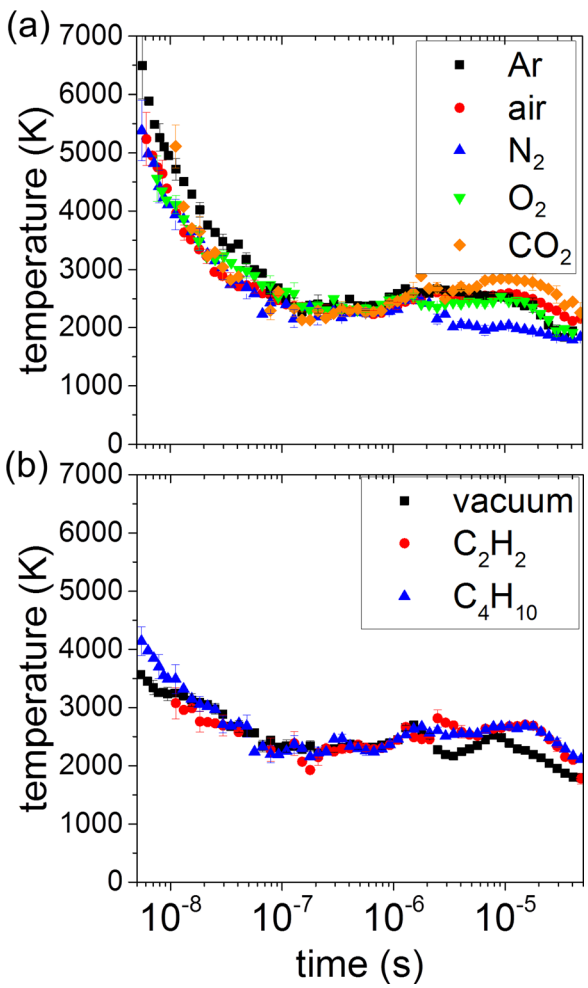

FIG. 4. Thermal histories from nXTX impacted at 2.8 km s^{-1} with pores filled with various gases. (a) The initial hot spot temperature was ~5500 K with the high C_p/C_v ratio gases Ar and the diatomics air, O_2, and N_2. (b) The hot spot temperature was ~4000 K with both the lower heat capacity ratio gases C_2H_4 and C_4H_{10} and under vacuum.

The tabletop shock compression system we developed, consisting of a km s^{-1} laser-driven flyer plate launcher, a shock target array with many identical EM charges, and a high-speed optical pyrometer, allowed us to conduct detailed studies of hot spots during shock the initiation of PETN-based EMs. The highest hot spot temperature of ~6000 K required microporosity of the PETN samples, as shown in experiments where we compared microporous PETN powder, vapor-deposited PETN, and XTX to a nanoporous XTX. In the nXTX, a hydraulic press was used to remove all pores larger than 1 μm, which caused the hot spot temperature to decrease to ~4000 K. In all cases, these initial high temperatures tapered off to ~2500 K in a few hundred nanoseconds without further temperature spikes. The thermal emission beyond 100 ns was attributed to deflagration ignited by hot spots.[30]

We have shown that the hot spots in both microporous and nanoporous charges resulted from the compression of gas inside shocked pores and that even under nominal vacuum, there is sufficient gas produced by the shock-induced decomposition of PETN to produce gas compression hot spots, as shown by comparison to the control $XTSiO_2$. The nonvolatile $XTSiO_2$ in vacuum did not produce any detectable hot spots, which proves the necessity of gas filled pores for the production of the hot spots. In the case of nanoporous EM, we found that the hot spot temperatures were dependent on the heat capacity ratio of the gas inside the pores. A simplified interpretation utilizing reversible adiabatic gas compression is consistent with both results. Our results indicate that in EM simulations, gas generation must be included in samples containing microstructures conducive to gas generation and compression in order to make accurate predictions of temperature histories. We note the similarities in hot spot generation from micropores in the compression of solids to cavitation in the collapse of bubbles in liquids, where cavitation is capable of developing hot spots in excess of 18,000 K.[37]

The research described in this study was based on the work supported by the U.S. Air Force Office of Scientific Research under awards FA9550-14-1-0142 and FA9550-16-1-0042, the U.S. Army Research Office under award W911NF-13-1-0217, and the Defense Threat Reduction Agency under award HDTRA1-12-1-0011. Belinda P. Johnson acknowledges support from the National Science Foundation Graduate Research Fellowship Program under Grant No. DGE – 1144245 and the Alfred P. Sloan Foundation's Minority Ph.D. (MPHD) Program, awarded in 2016.

[1]J. E. Field, Acc. Chem. Res. **25**(11), 489 (1992).
[2]W. P. Bassett and D. D. Dlott, Appl. Phys. Lett. **109**(9), 091903 (2016).

[3]W. P. Bassett and D. D. Dlott, J. Appl. Phys. **119**(22), 11 (2016).
[4]W. P. Bassett and D. D. Dlott, Rev. Sci. Instrum. **87**(10), 103107 (2016).
[5]M. D. Tarasov, I. I. Karpenko, V. A. Sudovtsov, and A. I. Tolshmyakov, Combust. Explos. Shock Waves **43**(4), 465 (2007).
[6]J. Köhler and R. Meyer, *Explosives*, 4th ed. (VCH Publishers, New York, 1993).
[7]L. E. Fried, in *Reviews in Computational Chemistry* edited by K. B. Lipkowitz and T. R. Cundari (Wiley, 2007), Vol. 25, pp. 159.
[8]T. M. Willey, K. Champley, R. Hodgin, L. Lauderbach, M. Bagge-Hansen, C. May, N. Sanchez, B. J. Jensen, A. Iverson, and T. van Buuren, J. Appl. Phys. **119**(23), 235901 (2016).
[9]R. Menikoff and T. D. Sewell, Combust. Theor. Model **6**(1), 103 (2002).
[10]H. K. Springer, C. M. Tarver, J. E. Reaugh, and C. M. May, in *18th Aps-Sccm and 24th Airapt, Pts 1-19*, edited by W. Buttler, M. Furlanetto, and W. Evans (IOP, 2014), Vol. 500.
[11]K. S. Vandersall, C. M. Tarver, F. Garcia, and S. K. Chidester, J. Appl. Phys. **107**(9), 094906 (2010).
[12]H. Golopol, N. Hetherington, and K. North, J. Hazard. Mater. **4**(1), 45 (1980).
[13]D. Stirpe, J. O. Johnson, and J. Wackerle, J. Appl. Phys. **41**(9), 3884 (1970).
[14]M. M. Chaudhri and J. E. Field, Proc. R. Soc. A. **340**(1620), 113 (1974).
[15]F. M. Najjar, W. M. Howard, L. E. Fried, M. R. Manaa, A. Nichols, and G. Levesque, in *Shock Compression of Condensed Matter - 2011, Pts 1 and 2*, edited by M. L. Elert, W. T. Buttler, and J. P. Borg *et al*. (AIP, 2012), Vol. 1426.
[16]A. Kapahi and H. S. Udaykumar, Shock Waves **23**(6), 537 (2013).
[17]T. R. Shan, R. R. Wixom, and A. P. Thompson, Phys. Rev. B. **94**(5), 054308 (2016).
[18]M. A. Wood, M. J. Cherukara, E. M. Kober, and A. Strachan, J. Phys. Chem. C **119**(38), 22008 (2015).
[19]L. Tran and H. S. Udaykumar, J. Propul. Power **22**(5), 959 (2006).
[20]N. K. Bourne and J. E. Field, Proc. R. Soc. Lond. A Mater. **435**(1894), 423 (1991).
[21]C. J. Wu, M. R. Manaa, and L. E. Fried, in *Materials Research at High Pressure*, edited by M. R. Manaa, A. F. Goncharov, R. J. Hemley *et al*. (Materials Research Society, 2007), Vol. 987, pp. 139.
[22]T. R. Shan, R. R. Wixom, A. E. Mattsson, and A. P. Thompson, J. Phys. Chem. B **117**(3), 928 (2013).
[23]A. Qi, W. A. Goddard, S. V. Zybin, J.-B. Andres, and T. Zhou, J. Phys. Chem. C **117**(50), 26551 (2013).
[24]S. V. Zybin, W. A. Goddard, P. Xu, A. C. T. van Duin, and A. P. Thompson, Appl. Phys. Lett. **96**(8), 081918 (2010).
[25]A. S. Tappan, R. Knepper, R. R. Wixom, M. P. Marquez, J. P. Ball, and J. C. Miller, in *Shock Compression of Condensed Matter - 2011, Pts 1 and 2*, edited by M. L. Elert, W. T. Buttler, J. P. Borg *et al*. (AIP, 2012), Vol. 1426.
[26]R. Knepper, A. S. Tappan, R. R. Wixom, and M. A. Rodriguez, J. Mater. Res. **26**(13), 1605 (2011).
[27]A. A. Banishev, W. L. Shaw, W. P. Bassett, and D. D. Dlott, J. Dyn. Behav. Mater. **2**(1), 194 (2016).
[28]A. D. Curtis, A. A. Banishev, W. L. Shaw, and D. D. Dlott, Rev. Sci. Instrum. **85**(4), 043908 (2014).
[29]T. C. Merkel, V. I. Bondar, K. Nagai, B. D. Freeman, and I. Pinnau, J. Polym. Sci. Part B: Polym. Phys. **38**(3), 415 (2000).
[30]C. M. Tarver, AIP Conf. Proc. **845**(1), 1026 (2006).
[31]S. Bastea, Sci. Rep. **7**, 42151 (2017).
[32]J. Kang, P. B. Butler, and M. R. Baer, Combust. Flame **89**(2), 117 (1992).
[33]J. Wang, W. P. Bassett, and D. D. Dlott, J. Appl. Phys. **121**(8), 085902 (2017).
[34]*CRC Handbook of Chemistry and Physics*, 97th ed. (CRC Press/Taylor & Francis, Boca Raton, FL, 2017).
[35]M. R. Manaa, E. J. Reed, L. E. Fried, G. Galli, and F. Gygi, J. Chem. Phys. **120**(21), 10146 (2004).
[36]B. L. Holian, T. C. Germann, J.-B. Maillet, and C. T. White, Phys. Rev. Lett. **89**(28), 285501 (2002).
[37]K. S. Suslick and D. J. Flannigan, Annu. Rev. Phys. Chem. **59**, 659 (2008).